HHS Public Access

Author manuscript

Adv Healthc Mater. Author manuscript; available in PMC 2022 August 31.

Published in final edited form as:

Adv Healthc Mater. 2016 March 09; 5(5): 593–601. doi:10.1002/adhm.201500697.

Reduced Blood Coagulation on Roll-to-Roll, Shrink-Induced Superhydrophobic Plastics

Jolie M Nokes[1], **Ralph Liedert**[2], **Monica Y Kim**[1], **Ali Siddiqui**[1], **Michael Chu**[1], **Eugene K Lee**[1], **Michelle Khine**[1]

[1]Department of Biomedical Engineering, University of California, Irvine, 3111 Engineering Hall, Irvine, CA, 92697, USA.

[2]VTT Technical Research Centre of Finland, 1 Kaitovayla, Oulu, 90570, Finland.

Abstract

The unique anti-wetting properties of superhydrophobic (SH) surfaces prevent the adhesion of water and bodily fluids, including blood, urine, and saliva. While typical manufacturable approaches to create SH surfaces rely on chemical and structural modifications, such approaches are expensive, require post-processing, and are often not biocompatible. In contrast, we demonstrate purely structural SH features are easily formed using high-throughput roll-to-roll (R2R) manufacturing by shrinking a pre-stressed thermoplastic with a thin, stiff layer of silver and calcium. These features are subsequently embossed into any commercially-available and FDA-approved plastic. The R2R SH surfaces have contact angles >150° and contact angle hysteresis <10°. Importantly, the surfaces minimize blood adhesion, leading to reduced blood coagulation without the need for anticoagulants. SH surfaces have >4200x reduction of blood residue area compared to the non-structured controls of the same material. In addition, blood clotting is reduced >5x using whole blood directly from the patient. Furthermore, these surfaces can be easily configued into 3-dimensional shapes, as we demonstrate SH tubes. With the simple scale-up production and the eliminated need for anticoagulants to prevent clotting, the proposed conformable SH surfaces can be impactful for a wide range of medical tools, including catheters and microfluidic channels.

Graphical Abstract

mkhine@uci.edu .

Supporting Information

Supporting Information is available from the Wiley Online Library or from the author.

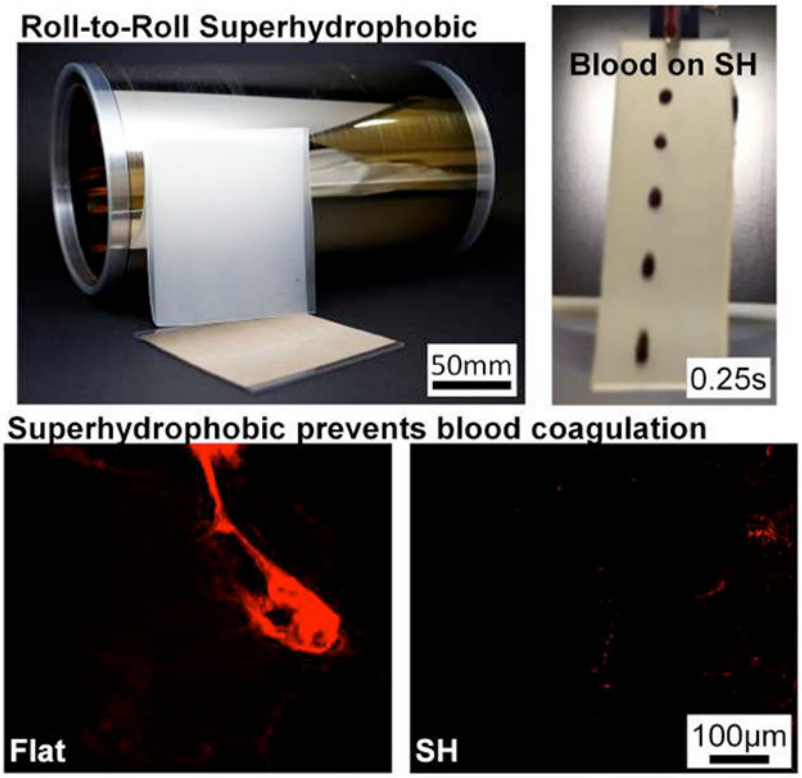

ToC: Superhydrophobic surfaces are achieved in a roll-to-roll platform by purely structural modification with no need for post-processing. The biocompatible superhydrophobic hard plastic prevents water, blood, urine, and saliva from adhering to the surface, and blood slides off with no residue. Blood coagulation is significantly reduced on the superhydrophobic surface compared to flat, and superhydrophobic tubes are easily configured for medical applications.

Keywords

superhydrophobic; roll-to-roll manufacturing; anticoagulation; blood clotting; biomaterial

1. Introduction

Superhydrophobic (SH) surfaces are attractive because of their self-cleaning, non-wetting, and anti-fouling properties.[1,2] The hierarchical micro- to nanoscale features characteristic of a SH surface effectively trap pockets of air between the surface and the applied fluid, causing minimal adhesion of the fluid to the surface[3] and allowing the droplet of fluid to glide across the peaks of the features with minimal friction.[4,5] SH surfaces have a contact angle (CA) greater than 150° and contact angle hysteresis (CAH) less than 10°.[3,6–8]

Due to their unique properties, SH surfaces have been used for bacterial prevention, drag reduction, non-adhesion, energy conservation, and green energy.[1,9–12] A SH surface has a low surface energy as well as micro- to nanoscale features, which are often achieved through a combination of chemical and structural modification. To lower the surface

energy, fluorocarbon and hydrocarbon chemicals can be deposited on roughened surfaces to achieve superhydrophobicity.[13–15] Additionally, surfaces with low surface energies can be structurally roughened using a variety of techniques such as plasma etching, chemical etching, lithography, sol-gel processing, laser ablation, electrospinning, crystallization, and oxidation.[5,15–20]

However, these production methods are often complex, expensive, serial, and require post-processing, preventing mass scale manufacturing.[1,10,11] Therefore, commercial applications of SH surfaces heretofore have been limited.[21,22] Furthermore, chemical additives are often not desirable for food or medical applications. A common mass manufacturing technique that yields high throughput is roll-to-roll (R2R) processing where alterations to a surface are performed in a single, quick process on a large roll of a material.[23,24] Originating from the printing industry, R2R manufacturing is currently widely used in printed electronics and printed diagnostics applications for high-volume, low-cost manufacturing of disposable components and can be performed in a variety of materials such as thin films, flexible polymers, and conformal tapes.[25] The ability to inexpensively manufacture large areas of SH surfaces without chemical modifications with high throughput and high fidelity would enable SH surfaces for a wide range of medical, healthcare, and consumer applications.

For example, blood clotting poses significant challenges for medical devices and clinical applications. In medical applications, the blood coagulation cascade is initially triggered by the intrinsic pathway when blood is exposed to a foreign surface such as glass or plastic.[26,27] Upon exposure, the protein Factor XII on the surface of platelets is activated by binding to the charged surface, in turn activating thrombin conversion to fibrin.[27–29] Thrombin polymerizes fibrinogen to form the non-globular protein fibrin that acts as glue in a blood clot, and the amount of fibrin correlates with the progression of blood clotting.[27] Fibrin networks are formed when strands of fibrin cross-link, and fibrin networks act as scaffolds for cells (such as platelets and fibroblasts) and blood clotting factors.[30–32] Blood clotting is then amplified by the adherence of platelets to fibrin networks, and additonal platelets are recruited to adhere, forming a hemostatic plug on a thrombogenic surface.[26,27,33] As fibrin networks form and platelets bind to fibrin, blood thickens and forms a blood clot within minutes.[34,35]

To prevent blood clotting in medical devices, anticoagulant drugs such as heparin and sodium citrate are pervasively used.[36–39] However, these drugs have drawbacks and may interfere with patient medication, medical procedures, or medical testing.[40–42] Alternatively, biomaterials have been used to prevent blood clotting by minimizing platelet adhesion and preventing the contact-activation pathway from being triggered.[26,43,44] SH surfaces have been shown to prevent the adhesion of protein and cells.[45–47] Further, SH surfaces have been shown to prevent platelet adhesion and therefore reduce blood coagulation.[37–39,43,44,48] Sun *et al.* has shown a reduction in platelet adherence to their SH surface and has also shown that platelets adhered to SH surfaces are less mature than platelets adhered to flat surfaces.[43] Further, Leslie *et al.* has shown a reduced fibrin network as well as reduced thrombosis under flow *in vitro* and *in vivo* on their SH surfaces.[36] Both these systems show that SH surfaces reduce the activation of blood clotting. Of

particular note, however, both systems use anticoagulants in their experiments and therefore have drawbacks to clinical applications. An ideal commercial device would obviate the use of anticoagulants altogether in order to be more compatible with clinical medicine.

The SH substrates introduced here could improve clinical medicine by preventing the blood coagulation cascade and preventing blood clotting of whole blood directly from the patient.[36] Because these SH surfaces can be imprinted into conformal tapes and thin films, they can be used to laminate various surfaces. Conversely, they can be imprinted directly into various FDA-approved plastics. The SH surfaces can be manufactured in a R2R platform with high throughput and high fidelity, and these substrates can realize important medical applications, for example, as catheters and medical tubing.

2. Results and Discussion

2.1. Sheet Evaporation Superhydrophobic Surfaces

We have previously developed SH surfaces by depositing a thin layer of silver and gold on our pre-stressed polymer.[9,49] Upon shrinking the pre-stressed polymer substrate, the mismatch in elastic moduli between the stiff metals and polymer yields a hierarchy of multi-scale features supportive of superhydrophobicity.[9,49] In this paper, we aim to scale-up manufacturing by depositing a thin layer of stiff material on the pre-stressed polymer in a R2R platform. Since gold was not a viable material to deposit R2R and because a bimetallic layer is necessary to form SH wrinkles, a combination of materials compatible with R2R deposition was first characterized in a sheet evaporation setup (data not shown). The deposition of silver (Ag) and calcium (Ca) on pre-stressed polystyrene (PS) was chosen as the optimal deposition materials, and the process flow of fabricating SH wrinkles in hard plastics is shown in Figure 1A.

To further optimize SH wrinkles, the deposition ratio of silver to calcium was characterized.[9,49] Figure 1B shows Scanning Electron Microscopy (SEM) images of the features from shrunk PS with 20nm Ag + 5nm Ca, 20nm Ag + 10nm Ca, 25nm Ag + 5nm Ca, 25nm Ag + 10nm Ca, 30nm Ag + 5nm Ca, and 30nm Ag + 10nm Ca deposited. All features yielded micro- to nanoscale structures, imprinted into hard plastics with high fidelity, and demonstrated superhydrophobicity. Supplemental Figure S1A graphs the 2D Fast Fourier Transforms (FFTs) and shows the spatial frequency of the SH features on the sheet evaporation to have the highest probability of wavelength between 714nm – 825nm.

Figure 1C–D graph the CA and CAH of water, urine, saliva, and blood on the six deposition conditions molded and embossed into the hard plastic polypropylene (PP). Water has a CA greater than 150° for all substrates, and the CA of water ranges from 158° ± 4° to 161° ± 5°. Urine, saliva, and blood also have SH CA values on the six different deposition conditions. CA values of urine range from 149° ± 8° to 152° ± 7°. CA values of saliva range from 148° ± 8° to 156° ± 4°. CA of blood range from 148° ± 6° to 154° ± 4°. Note that standard deviations overlap, and conditions are not statistically different.

CAH values were measured by taking the difference in advancing and receding CA values. CAH values are also indicative of superhydrophobicity for water, urine, saliva, and blood.

CAH values for water range from 6° ± 2° to 9° ± 4°. CAH values for urine range from 5° ± 1° to 9° ± 2°. CAH values for saliva range from 4° ± 1 to 6° ± 1°. CAH values for blood range from 6° ± 1° to 8° ± 2°.

The 20nm Ag + 5nm Ca deposition was chosen as the optimal condition because superhydrophobicity is consistently achieved for all fluids (i.e. CA >150° and CAH <10°). The 20nm Ag + 5nm Ca deposition also requires the least amount of materials and is the most beneficial for manufacturing.

2.2. Roll-to-Roll Superhydrophobic Surfaces

Next, R2R deposition on pre-stressed PS was performed, and SH features were created in a R2R platform. Figure 2A shows the process flow of R2R production. Silver and calcium are deposited on a pre-stressed roll of PS. Sections of the roll are shrunk, and the SH features are imprinted into silicones and hard plastics as the final product. Figure 2B–C show the R2R deposition equipment and the actual size of the metalized roll, shrunk master, and molded PP product. The fidelity of the roll was tested by characterizing the front, middle, and rear of the roll.

Figure 2D shows the SEMs of the mico- to nanoscale features of the front, middle, and rear of the roll. Features are consistent throughout the roll, and therefore metal deposition and superhydrophobicity are consistent throughout the roll. Supplemental Figure S1B graphs the 2D FFTs of the spatial frequency of the SH features on the R2R deposition. Supplemental Figure S1C overlays the 20nm Ag + 5nm Ca FFT from the sheet evaporation with the FFT data for the front, middle, and rear of the R2R roll. The front, middle, and rear of the R2R depositions have the highest probability of wavelength between 714nm – 825nm. In addition, the wavelength distribution of the R2R sample is similar to the sheet evaporation wavelength distribution.

Figure 2E–F graph the CA and CAH values for water, urine, saliva, and blood tested on the front, middle, and rear of the roll. CA and CAH values for water and bodily fluids are indicative of superhydrophobicity. The average CA values are 162° ± 5° for water, 158° ± 6° for urine, 154° ± 6° for saliva, and 154° ± 5° for blood.

CAH values average 6° ± 1° for water, 7° ± 1° for urine, 7° ± 1° for saliva, and 9° ± 2° for blood. The standard deviation of the front, middle, and rear of the roll overlap for CA and CAH values for each fluid, confirming that superhydrophobicity is consistent throughout the roll. Note that CAH values for saliva on the R2R surfaces are greater than CAH values on the sheet evaporation surfaces. The surface tension of saliva, however, is shown to fluctuate between 45mNm^{-1} to 69mNm^{-1} depending on when subjects drank water prior to collection and also the time of testing post collection.[50] The CA and CAH can be dramatically affected by such fluctuation but notably, values are consistently indicative of superhydrophobicity on the R2R surfaces.

2.3. Blood Adherence

Figure 3 shows the behavior of blood on a SH surface compared to a flat surface. Multiple drops of blood are required for a droplet to slide off the 1”×3” flat strip (within 15 seconds),

and visually, a significant amount of blood residue is smeared on the flat surface. Blood slides off the 1”×3” SH strip within 0.25 seconds and visually, no blood sticks to the SH surface. Videos of the droplets of blood sliding off the flat and SH surfaces are shown in the Supporting Information (Supplemental Figure S2 and Supplemental Figure S3). Visually, more blood adheres to the flat surface than the SH surface.

Figure 3C–D measure the amount of blood residue area and volume adhered to a flat surface compared to a SH surface. The area of blood residue on the flat surface is 21 ± 5% and is within the noise for the SH surface (0.005 ± 0.004%), which is a more than 4200x reduction of blood area adherence. Blood residue volume on the SH and flat surfaces is measured using a phenol-blood assay. A standard dilution curve is created using dilutions of blood (Supplemental Figure S4), and the absorbance values for blood residue volume are compared to the standard curve. 80 ± 15% of blood volume sticks to the flat surface compared to only 3 ± 2% of blood volume sticks to the SH surface, which is more than 28x reduction compared to flat and more than 35x reduction of overall blood volume adherence.

2.4. Blood Coagulation

SH surfaces are shown to prevent blood coagulation using blood directly from the patient (i.e. without anticoagulants). Figure 4 shows the amount of fluorescently-labeled fibrin on the flat and SH surfaces, indicating the amount of blood clotting. Within the first 10min of incubation, the SH surfaces have significantly less blood clotting area compared to the flat surfaces, and the trend continues for the 20 – 50min incubation times. Clotting area is reduced >170x for the initial 10min incubation time and is reduced >27x for the 20min and 30min incubation times. By the 40 – 50min incubation times, clotting is reduced 5x on the SH surfaces compared to flat. Blood coagulation is delayed on the SH surfaces due to the decrease in contact activation. Figure 4A pairs images of fluorescently-labeled fibrin with the data quantified in Figure 4B as the percent area of the fibrin clot.[48] Further, our SH surfaces use whole blood directly from the patient and negate the need for anticoagulants.

Figure 5 shows SEM images of the 10 – 50min blood coagulation incubation times as well as controls without blood coagulation for the flat and SH surfaces. Platelets begin to mature and fibrin networks begin to form by the 20min incubation time on the flat surfaces. By 30min, platelets are maturing and fibrin networks are apparent. Platelets continue to mature, and fibrin networks continue to grow at 30 – 50min incubation times on the flat surfaces. On the SH surface, however, platelets remain immature at the 40min incubation time and by 50min, platelets begin to mature and spread along the peaks of the micro surfaces. Fibrin networks are seen at the 30min incubation time on SH surfaces and continue to form in the 40min and 50min incubation times. The fibrin networks form on the peaks of the micro structures, and platelets and fibrin span the micro valleys and attach to the micro peaks on the SH surfaces. By the 50min incubation time on the SH surfaces, some blood clotting has occurred, but clotting has been significantly reduced compared to flat surfaces due to the minimal adhesion which delays the contact-activation pathway. Overall, SH surfaces have reduced fibrin network formation and platelet maturation on their surface compared to flat.

2.5 Rolled Superhydrophobic Tubing

The R2R metalized masters are conformal during the shrinking process, and rolled SH tubes are created, as shown in Figure 6. SH features are achieved on the inner and outer circumference of the tubes, and various diameters of tubes are achieved for various applications. The SH features are subsequently molded into polydimethylsiloxane (PDMS) to achieve SH rolled tubes of various diameters. Fluid slides through the flat and SH tubes (Supplemental Figure S5 and Supplemental Figure S6), and no residue remains on the SH tube, while fluid adheres to the flat tube. Due to the anticoagulant nature of the SH features and the conformability of the metalized PS master, the SH surfaces have potential for medical materials such as catheters, medical tubing, and microfluidic tubing. Such tubing could prevent blood clotting and tubing clogging for medical applications.

3. Conclusion

SH surfaces are created in a R2R platform with high fidelity and high throughput. The purely structural modification allows for inexpensive embossing into any commercially-available and FDA-approved plastic for medical applications, and post processing is not necessary. The SH surfaces are phobic to water, blood, urine, and saliva. Blood residue area is reduced >4200x, and blood residue volume is reduced >28x on the SH compared to flat. Blood coagulation is reduced >5x after 50min incubation, and platelet and fibrin network formation are less mature on a SH surface compared to the nonstructured flat counterpart. The anticoagulant nature of the SH surfaces negates the need for anticoagulants, broadening the potential medical applications of the SH surfaces. In addition, the SH surfaces can be conformal, and the SH features can be rolled into tubes. The SH features can be created on the inner or outer perimeter of the tube and molded into silicones for fluid flow with minimal adhesion on the surface. The SH plastics are biocompatible, reduce blood coagulation, and are conformal to 3-dimensional shapes. By obviating the need for anticoagulants and with the simple scale-up production method presented, our SH surfaces can be impactful for a wide range of medical tools and applications.

4. Experimental Section

Sheet Evaporation and Roll-to-Roll Superhydrophobic Surfaces:

To achieve R2R SH surfaces, the deposition materials and the thickness of deposition materials were first characterized in a sheet process to match the hierarchical wrinkles of the small scale SH surfaces described previously.[9,49] Silver and calcium were chosen as deposition materials because of their high Young's modulus, and the ratio of silver to calcium was optimized to yield hierarchical micro- to nanoscale features in the SH regime. Sheets of pre-stressed PS were cut to fit the sheet evaporation chamber, and 20nm Ag + 5nm Ca, 20nm Ag + 10nm Ca, 25nm Ag + 5nm Ca, 25nm Ag + 10nm Ca, 30nm Ag + 5nm Ca, and 30nm Ag + 10nm Ca were deposited using thermal vacuum deposition (MBRAUN MB-ProVap, Germany). Silver was deposited first, then calcium.

Once deposition conditions were determined, 20nm + 5nm Ca was deposited in a single process on the pre-stressed PS in a R2R platform using thermal evaporation (VTT EVA

R2R Evaporator, Finland). A roll of pre-stressed PS was mounted on a feeding roller, and silver and calcium were deposited simultaneously (with a spacer wall to prevent mixing) under vacuum at a constant web feeding rate. Deposition rate and thickness were monitored (Sycon STM-2, USA). Silver and calcium were deposited on the entire roll, and the roll was characterized for deposition integrity.

The SH features created during the shrinking process were molded into silicones and subsequently embossed into hard plastics. Silver and calcium have a strong adhesion to the PS shrink film after the shrinking process, and the materials do not transfer to the final plastic product during the molding and embossing steps. Due to the structural nature of the SH surfaces (embossed), SH features are as robust and stable as the initial plastic material. For example, SH PP has the same inherent properties as flat PP (such as glass transition temperature), but the SH nature alters the interaction of the plastic with fluid, allowing the surface to prevent adhesion.

Fluids:

Ultrapure water (Millipore, USA) was used. Urine, saliva, and blood were collected from voluntary subjects. Urine and saliva were collected from patients and used directly on the surfaces. For the CA, CAH, and blood adherence measurements, whole blood was collected by venipuncture in glass tubes with sodium citrate as the anticoagulant to prevent blood clotting. For the blood coagulation studies, whole blood was collected by venipuncture in glass tubes without anticoagulants. Whole blood directly from the patient was used within 2min of collection to prevent premature clotting. During the CA, CAH, and blood adherence measurements, blood with the anticoagulant sodium citrate is used in order to keep the blood from clotting during characterization. Since blood without anticoagulants clots within minutes, anticoagulants are necessary to characterize the fluid behavior of blood on the surfaces prior to coagulation studies.

Contact Angle and Contact Angle Hysteresis Measurements:

5μL of fluid was pipetted on the surfaces to measure CA. Droplet images were taken using a Canon EOS Rebel Camera and a macro lens perpendicular to the surface. CA values were measured using the low-bond axisymmetric drop shape analysis (LB-ADSA) software in ImageJ.[51] CAH values were measured using a drop shape analyzer (Kruss DSA30, Germany) and Advance software by taking the difference of the advancing and receding CA. 10μL or 20μL of fluid was deposited and retracted on the surface at a constant rate to measure the advancing and receding CA. Data was analyzed using Excel. N=9

Blood Adherence Area and Volume:

Flat PP and embossed SH PP samples were cut into 1”×3” strips and placed at a 30° angle. Images were taken of the surface prior to the addition of whole blood to subtract background. Next, 200μL of citrated whole blood was deposited at the top of the strip and allowed to naturally slide off. Images were taken post blood deposition, and all images were processed in ImageJ to determine the area of blood adhesion. Area was calculated by thresholding the background and calculating the area of coverage on the surface.

To determine trace amounts of blood residue volume, 200μL of citrated blood was deposited on the 1”×3” flat and SH strips at a 30° angle. Residual blood was collected from the strips, and the Kastle-Meyer test was performed in well plates. Phenolphthalein (phph) was added (TriTech Forensics, USA), and a colorimetric shift occurs in the presence of hemoglobin (i.e. blood). The colorimetric shift was characterized using a plate reader (Biorad Benchtop Microplate Reader, USA) to measure absorbance values (at 570nm). Absorbance values of blood dilutions were characterized and used as the standard curve. The amount of blood residue volume on the samples was determined by comparing the absorbance values of the samples to the absorbance values of the standard curve. N=6

Blood Coagulation:

Flat PP and embossed SH PP samples were cut to 6mm diameter circles using a CO2 laser cutter (Versa Laser, USA) and adhered to a dish using double sided tape. Samples were cleaned with pressurized air. Whole blood was collected by venipuncture in glass tubes without anticoagulants. 50μL of blood was immediately added to the flat and SH surfaces (within 2min of collection), and conditions are consistent for flat and SH samples. Fibrinogen labeled with Alexa Flour 647 (Invitrogen, USA) was added to blood at a 150μgmL^{-1} concentration. Samples were covered with foil and incubated for 10min, 20min, 30min, 40min, and 50min. The blood was removed from the substrates, and the substrates were rinsed with phosphate buffer solution (PBS, Sigma Aldrich, USA). Fluorescent images were taken with a Cy5 filter on an upright microscope (Olympus BX53, Japan) and high speed digital camera (Hamamatsu C11440, Japan). Fibrin clot percent area was calculated in MATLAB® by thresholding out the background signal and measuring the percent area of fluorescently-labeled fibrinogen, as shown previously.[36] N=9

Scanning Electron Microscopy:

Substrates were sputtered with 7nm of iridium to prevent charging. An FEI Magellan 400L XHR SEM (FEI, USA) was used to image. 1–3kV was used to view the substrates. Prior to taking SEM images, blood coagulation samples were fixed with 1.5% glutaraldehyde (Fisher Scientific, USA), 0.07M sodium cacodylate (CAC, Sigma-Aldrich, USA), and 3mM magnesium chloride (MgCl2, Sigma-Aldrich, USA). The samples were rinsed with 0.1M CAC, 3mM MgCl2, and 2.5% sucrose (Sigma-Aldrich, USA) and post-fixed with 1% osmium tetroxide (OsO4, Sigma-Aldrich, USA), 0.8% potassium hexacyanoferrate(II) trihydrate (K4Fe(CN)6, Sigma-Aldrich, USA), and 0.1M CAC. The samples were dehydrated with graduations of ethanol, then hexamethyldisilazane (HMDS, Sigma-Aldrich, USA).

Two-Dimensional Fast Fourier Transform (2D FFT):

The wavelength distribution of the wrinkles was found by applying a 2D FFT on SEM images of the SH surfaces using MATLAB®. The power spectral density (PSD) from the 2D FFT and was shifted so that the zero wavenumber (1/wavelength) was centered. To create a plot of wavenumber versus intensity, the PSD was integrated over theta for increasing value of wavenumber; this resulted in a cumulative distribution curve of the wavenumber for this sample. The percent distribution of the wavenumber was then calculated by taking the derivative of the cumulative distribution function. The intensity for the wavenumbers

corresponding to wavelengths greater than the scale bar of the SEM images was attenuated to better see the larger wavenumbers. The curve was smoothed with a running average and the maximum value was normalized to one to give the relative intensity of the wrinkles versus their wavelength.

Rolling Superhydrophobic Tubes:

A section of pre-shrunk metalized PS was cut to size (based on the desired final tubing dimensions) and rolled into a tube. The seam of the PS roll was sealed with a heat sealer (Impulse Sealer, USA) to control uniform shrinking, and a heat resistant mold (such as a glass or metal rod) with the desired final dimensions was inserted inside the unshrunk, metalized, and rolled PS tube. The metalized PS was heated to 350°F in a conventional convection oven (Black and Decker, USA), and the metalized PS conforms to the mold upon shrinking. The SH features can be on the inner or outer circumference of the tube. The PS tubes were molded with polydimethylsiloxane (PDMS) to achieve SH tubes and cylinders in polymers. Droplets of yellow food dye were dropped in the tubes and allowed to slide off.

Supplementary Material

Refer to Web version on PubMed Central for supplementary material.

Acknowledgements

This work was funded in part by the National Institute of Health (NIH) Director's New Innovator Award (award number OD007283-01), National Science Foundation and the industrial members of the Center for Advanced Design and Manufacturing of Integrated Microfluidics (NSF CADMIM award number IIP-1362165), VTT Technical Research Centre of Finland, and Summer Undergraduate Research Program (SURP).

References

[1]. Ma M, Hill RM, Curr. Opin. Colloid Interface Sci 2006, 11, 193.

[2]. Zhang Y-L, Xia H, Kim E, Sun H-B, Soft Matter 2012, 8, 11217.

[3]. Cassie BD, Baxter S, Trans. Faraday Soc 1944, 40, 546.

[4]. Lafuma A, Quéré D, Nat. Mater 2003, 2, 457. [PubMed: 12819775]

[5]. Ma M, Hill RM, Lowery JL, Fridrikh SV, Rutledge GC, Langmuir 2005, 21, 5549. [PubMed: 15924488]

[6]. Gao L, McCarthy TJ, Langmuir 2006, 22, 6234. [PubMed: 16800680]

[7]. McHale G, Aqil S, Shirtcliffe NJ, Newton MI, Erbil HY, Langmuir 2005, 21, 11053. [PubMed: 16285771]

[8]. McHale G, Shirtcliffe NJ, Newton MI, Langmuir 2004, 20, 10146. [PubMed: 15518506]

[9]. Freschauf LR, McLane J, Sharma H, Khine M, Shrink-Induced Superhydrophobic and Antibacterial Surfaces in Consumer Plastics. PLoS One 2012, 7, 1.

[10]. Bhushan B, Jung YC, Prog. Mater. Sci 2011, 56, 1.

[11]. Nosonovsky M, Bhushan B, Curr. Opin. Colloid Interface Sci 2009, 14, 270.

[12]. Liu M, Wang S, Wei Z, Song Y, Jiang L, Adv. Mater 2009, 21, 665.

[13]. Lu X, Zhang C, Han Y, Macromol. Rapid Commun 2004, 25, 1606.

[14]. Chu Z, Seeger S, Chem. Soc. Rev 2014, 43, 2784. [PubMed: 24480921]

[15]. Shiu J-Y, Kuo C-W, Chen P, Proc. SPIE 2004, 5648, 325.

[16]. Qian B, Shen Z, Langmuir 2005, 21, 9007. [PubMed: 16171323]

[17]. Fürstner R, Barthlott W, Neinhuis C, Walzel P, Langmuir 2005, 21, 956. [PubMed: 15667174]

[18]. Shirtcliffe NJ, McHale G, Newton MI, Perry CC, Langmuir 2003, 19, 5626.

[19]. Baldacchini T, Carey JE, Zhou M, Mazur E, Langmuir 2006, 22, 4917. [PubMed: 16700574]

[20]. Feng X, Feng L, Jin M, Zhai J, Jiang L, Zhu D, J. Am. Chem. Soc 2004, 126, 62. [PubMed: 14709060]

[21]. Kobrin Rolith, Nanostructures with Anti-Counterfeiting Features and Methods of Fabricating the Same 2011.

[22]. Smith JD, LiqiGlide, Non-Toxis Liquid Impregnated Surfaces. Can. Med. Assoc. J 2015.

[23]. Liedert R, Amundsen LK, Hokkanen A, Mäki M, Aittakorpi A, Pakanen M, Scherer JR, Mathies R. a., Kurkinen M, Uusitalo S, Hakalahti L, Nevanen TK, Siitari H, Söderlund H, Lab Chip 2012, 12, 333. [PubMed: 22127494]

[24]. Roll to Roll (R2R) Processing Technology Assessment.

[25]. Peng L, Deng Y, Yi P, Lai X, J. Micromechanics Microengineering 2014, 24, 013001.

[26]. Mackman N, Tilley RE, Key NS, Arterioscler. Thromb. Vasc. Biol 2007, 27, 1687. [PubMed: 17556654]

[27]. Furie B, Furie BC, Cell 1988, 53, 505. [PubMed: 3286010]

[28]. Cool DE, Macgillivray R. T. a, 1987, 262, 13662.

[29]. Stavrou E, Schmaier AH, Thromb. Res 2010, 125, 210. [PubMed: 20022081]

[30]. Campbell RA, Overmyer KA, Selzman CH, Sheridan BC, Wolberg AS, Blood 2009, 114, 4886. [PubMed: 19797520]

[31]. Collet JP, Park D, Lesty C, Soria J, Soria C, Montalescot G, Weisel JW, Arterioscler. Thromb. Vasc. Biol 2000, 20, 1354. [PubMed: 10807754]

[32]. Chernysh IN, Weisel JW, Dc W, Network 2011, 111, 4854.

[33]. Heemskerk JWM, Bevers EM, Lindhout T, Thromb. Haemost 2002, 88, 186. [PubMed: 12195687]

[34]. Mustard JF, Packham MA, Br. Med. Bull 1977, 33, 187. [PubMed: 334317]

[35]. Pešáková V, Kubies D, Hulejová H, Himmlová L, J. Mater. Sci. Mater. Med 2007, 18, 465. [PubMed: 17334697]

[36]. Leslie DC, Waterhouse A, Berthet JB, Valentin TM, Watters AL, Jain A, Kim P, Hatton BD, Nedder A, Mullen K, Super EH, Howell C, Johnson CP, Vu TL, Rifai S, Hansen A, Aizenberg M, Super M, Aizenberg J, Ingber DE, Nat. Biotechnol 2014, 32, 1134. [PubMed: 25306244]

[37]. Zhang Z, Borenstein J, Guiney L, Miller R, Sukavaneshvar S, Loose C, Lab Chip 2013, 13, 1963. [PubMed: 23563730]

[38]. Hou X, Wang X, Zhu Q, Bao J, Mao C, Jiang L, Shen J, Colloids Surfaces B Biointerfaces 2010, 80, 247. [PubMed: 20630719]

[39]. Mao C, Liang C, Luo W, Bao J, Shen J, Hou X, Zhao W, J. Mater. Chem 2009, 19, 9025.

[40]. Power A, Duncan N, Singh SK, Brown W, Dalby E, Edwards C, Lynch K, Prout V, Cairns T, Griffith M, McLean A, Palmer A, Taube D, Am. J. Kidney Dis 2009, 53, 1034. [PubMed: 19394731]

[41]. Renzi R, Finkbeiner S, Am. J. Emerg. Med 1991, 9, 551. [PubMed: 1930395]

[42]. Walenga JM, Bick RL, Curr. Concept Thromb 1998, 82, 635.

[43]. Sun T, Tan H, Han D, Fu Q, Jiang L, Small 2005, 1, 959. [PubMed: 17193377]

[44]. Zhou M, Yang JH, Ye X, Zheng AR, Li G, Yang PF, Zhu Y, Cai L, J. Nano Res 2008, 2, 129.

[45]. Koc Y, de Mello a J., McHale G, Newton MI, Roach P, Shirtcliffe NJ, Lab Chip 2008, 8, 582. [PubMed: 18369513]

[46]. Alves NM, Shi J, Oramas E, Santos JL, Tomás H, Mano JF, J. Biomed. Mater. Res. - Part A 2009, 91, 480.

[47]. Luong-Van E, Rodriguez I, Low HY, Elmouelhi N, Lowenhaupt B, Natarajan S, Lim CT, Prajapati R, Vyakarnam M, Cooper K, J. Mater. Res 2012, 28, 165.

[48]. Leslie DC, Waterhouse A, Berthet JB, Valentin TM, Watters AL, Jain A, Kim P, Hatton BD, Nedder A, Mullen K, Super EH, Howell C, Johnson CP, Vu TL, Rifai S, Hansen A, Aizenberg M, Super M, Aizenberg J, Ingber DE, Nat. Biotechnol 2014, submitted, 93.

[49]. McLane J, Wu C, Khine M, Adv. Mater. Interfaces 2015, 2, 1.

[50]. Kazakov VN, Udod AA, Zinkovych II, Fainerman VB, Miller R, Colloids Surfaces B Biointerfaces 2009, 74, 457. [PubMed: 19577904]

[51]. Stalder AF, Melchior T, Müller M, Sage D, Blu T, Unser M, Colloids Surfaces A Physicochem. Eng. Asp 2010, 364, 72.

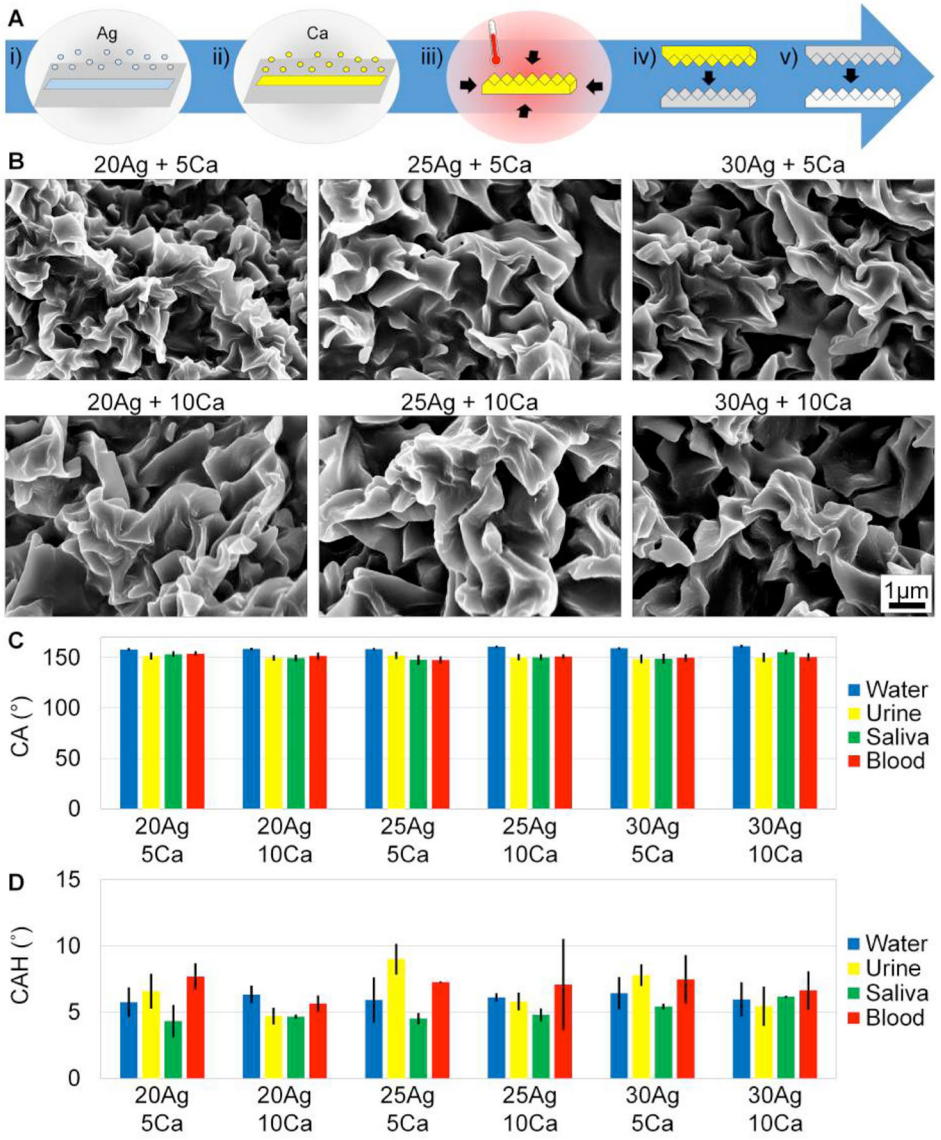

Figure 1:

Sheet evaporation on PS was characterized with 20nm Ag + 5nm Ca, 20nm Ag + 10nm Ca, 25nm Ag + 5nm Ca, 25nm Ag + 10nm Ca, 30nm Ag + 5nm Ca, and 30nm Ag + 10nm Ca. A) i) Silver is first deposited, ii) then calcium is deposited in sheet evaporation. iii) The SH features are formed while shrinking the metalized film, and the SH features are iv) molded into an intermediary silicone and v) embossed into plastic to achieve the final product. B) SEM images of the hierarchical features in plastic show hierarchical winkles. Scale bars are 1μm for all images. C) CA of water and bodily fluids on all conditions are SH. D) CAH of water and bodily fluids on all conditions are SH.

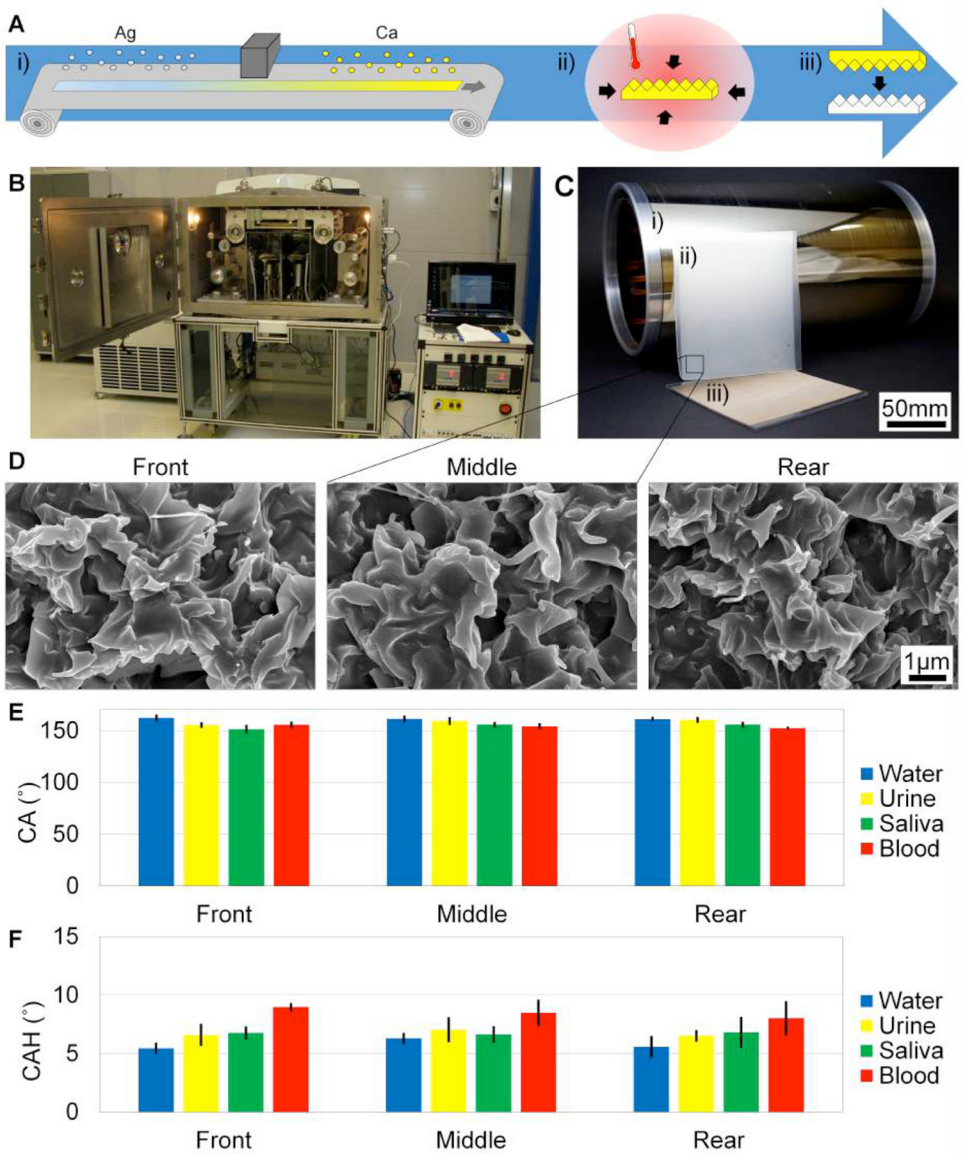

Figure 2:

SH surfaces are fabricated in a R2R platform. A) i) 20nm Ag, then 5nm Ca are deposited on the pre-stressed PS film in a R2R deposition chamber, ii) the metalized PS shrink film is shrunk to achieve SH features, and iii) the SH features are imprinted into hard plastics. B) Materials are deposited on the shrink film in the VTT EVA R2R Evaporator Line. C) (i) A roll of metalized shrink film is 30cm × 300m. (ii) The metal film is shrunk), and (iii) large SH hard plastics are created. D) SEM images of the front, middle, and rear of the metalized PS roll were tested to show the consistency of deposition throughout the roll. Scale bars are 1μm for all SEM images. E) CA of water, urine, saliva, and blood on all conditions are SH. F) CAH of all fluids are SH on all conditions.

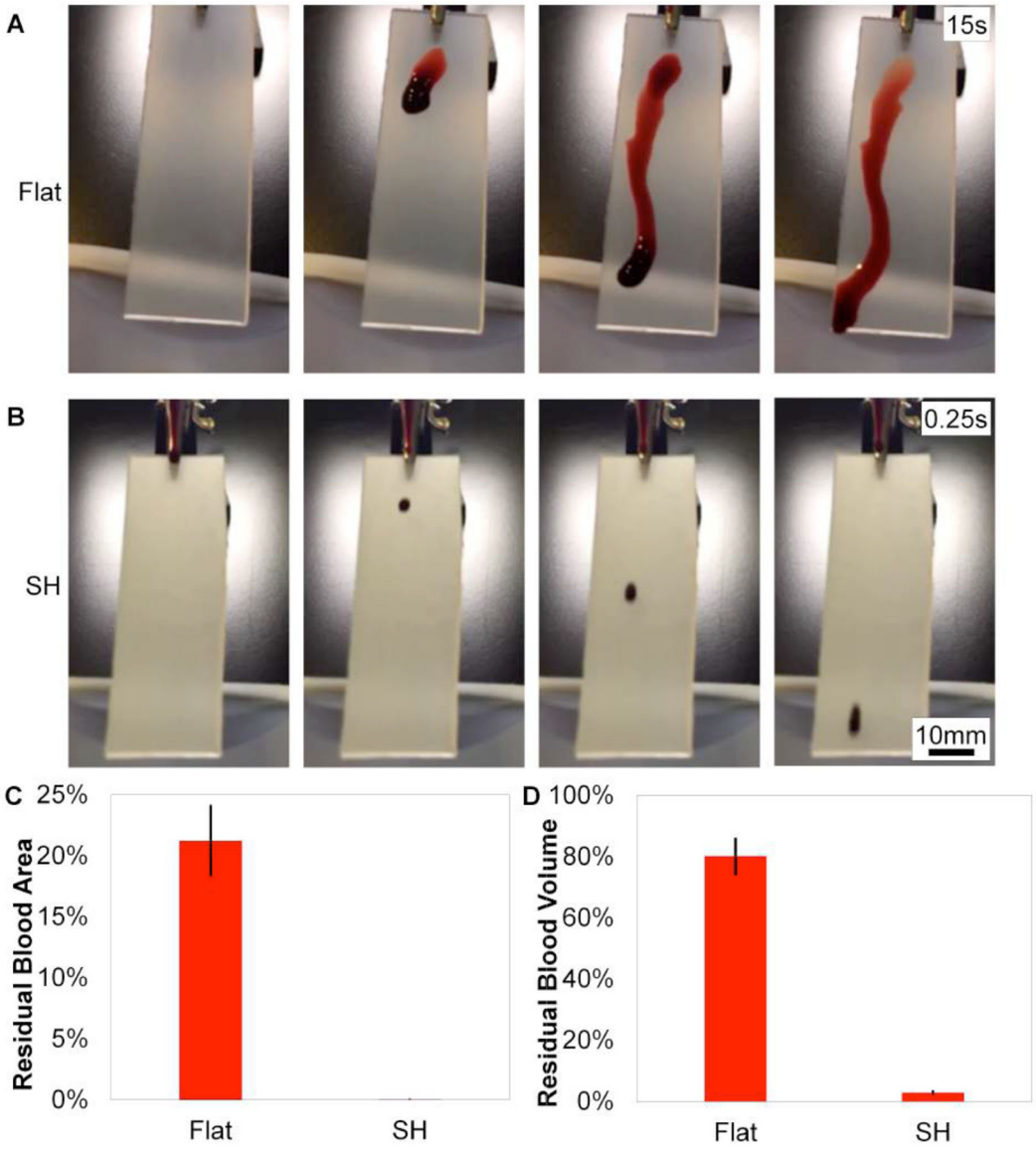

Figure 3:

Still images of blood sliding on flat and SH PP are taken with a high speed camera. A) Multiple drops of blood are required for blood to slide off the flat surface. Blood smears and partially slides off the flat surface within 15 seconds. B) One droplet of blood completely slides off the SH surface within 0.25 seconds and leaves no visual residue. Scale bar is 10mm for flat and SH. C) Blood residue area is reduced >4200x on the SH surface compared to flat. D) Significantly less blood volume adheres to the SH surface compared to flat (>28x).

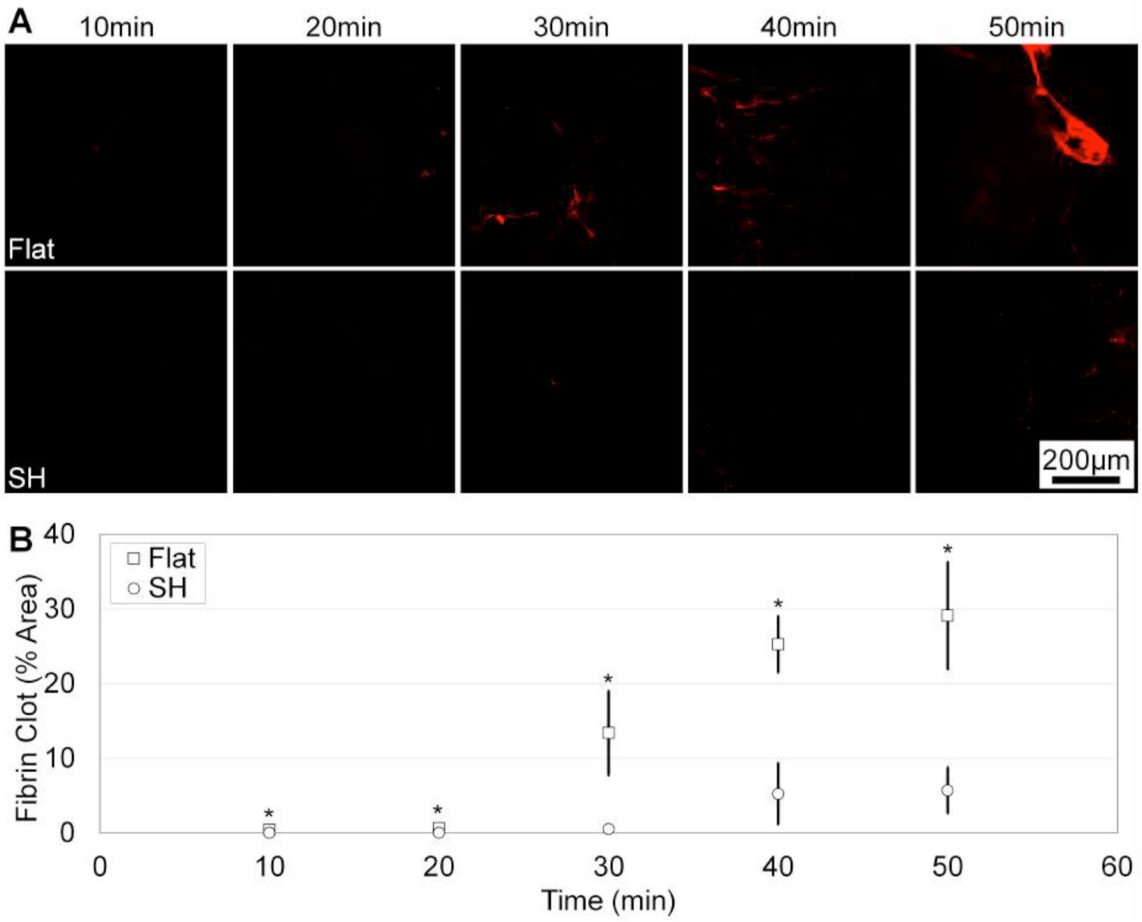

Figure 4:

Blood coagulation is reduced on SH surfaces compared to flat. A) Fluorescently-labeled fibrinogen indicates blood coagulation on flat (top) and SH (bottom) surfaces. Scale bar is 200μm. B) SH surfaces have significantly less blood coagulation compared to flat (>5x reduction at 50min).

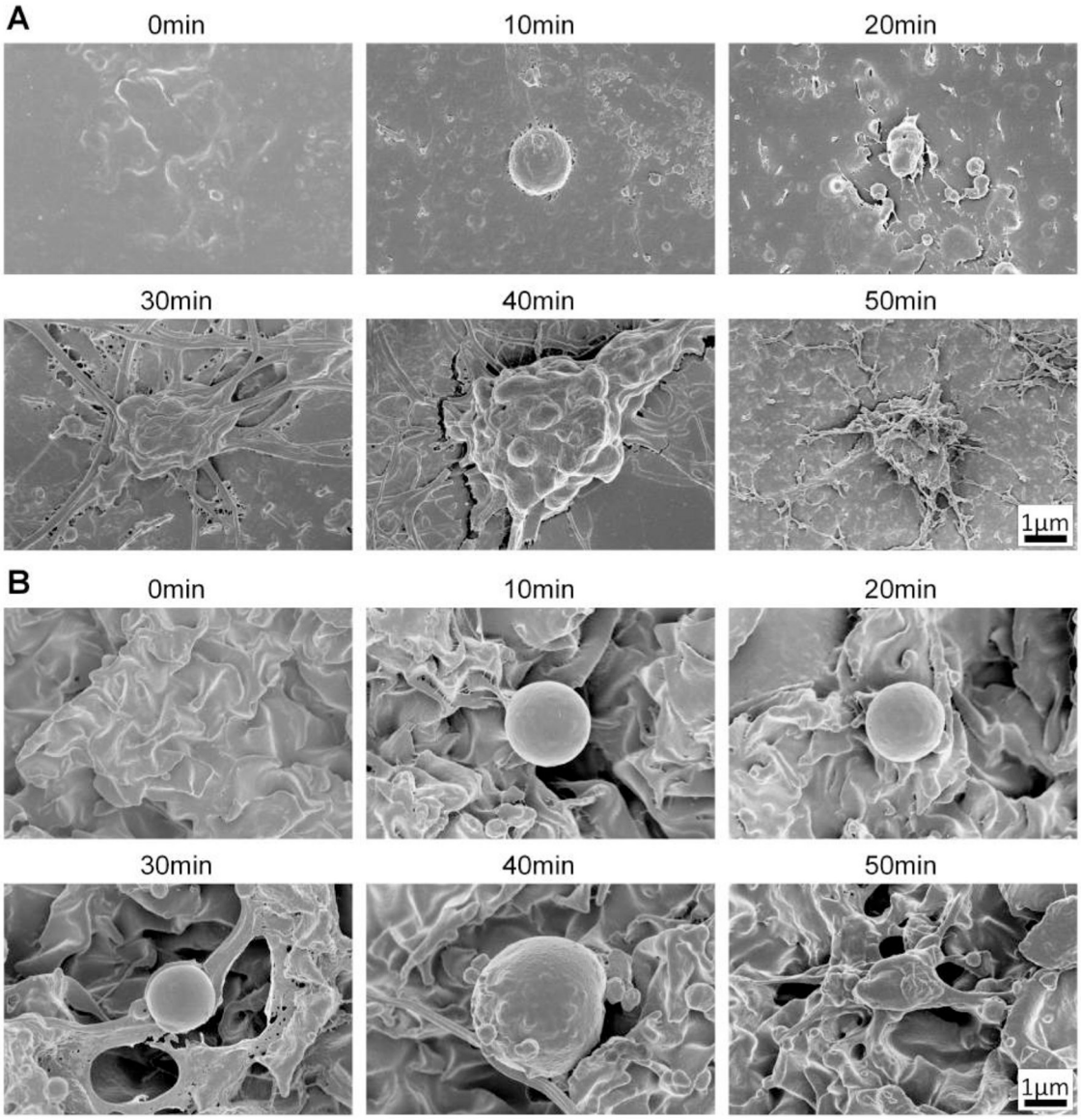

Figure 5:

SEM images of blood coagulation on flat and SH PP for 0–50min time points. A) Flat surfaces show platelet maturation and fibrin formation within the first 20min of incubation. B) SH surfaces have less mature platelets up to 40min and fibrin formation is less prominent at the lower time points. Scale bars are 1μm for all images.

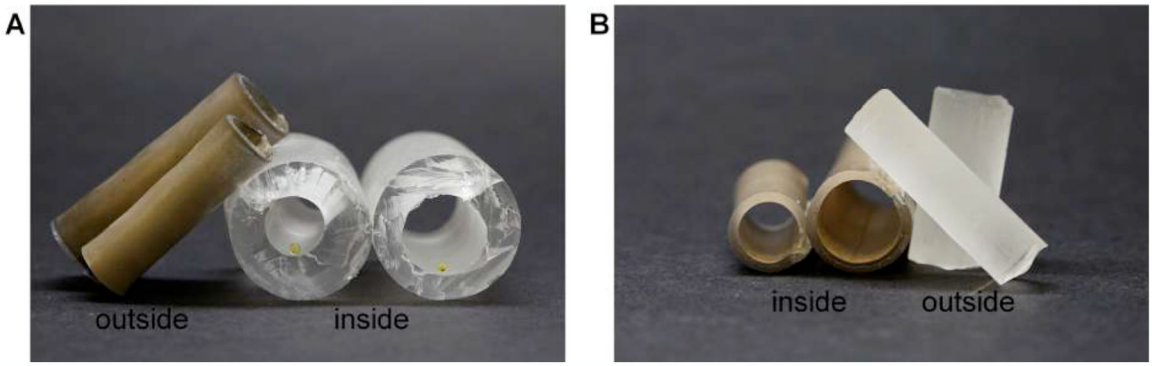

Figure 6:

Metalized PS sheets are shrunk as rolled tubes with varying diameters. A) SH features are formed on the outside of the rolled PS, and when PDMS molds the features, SH PDMS tubes with features on the inside are created. Droplets of yellow food dye inside the tube have SH CA values. B) SH features are formed on the inside of the rolled PS, and when PDMS molds the features, SH cylinders with SH features on the outside are created.